J Appl Electrochem (2012) 42:139–144
DOI 10.1007/s10800-012-0380-x

ORIGINAL PAPER

High cyclic performance of V_2O_5@PPy composite as cathode of recharged lithium batteries

Hongbin Zhao · Anbao Yuan · Bingdi Liu · Siyi Xing · Xiaoyan Wu · Jiaqiang Xu

Received: 27 September 2011 / Accepted: 20 January 2012 / Published online: 2 February 2012

Abstract Micro–nanosized vanadium pentoxide (V_2O_5) was synthesized by hydrothermal reduction of amorphous V_2O_5, followed by thermal treatment in air atmosphere. Pyrrole was in-situ polymerization on the surface of V_2O_5 to obtain V_2O_5@PPy hybrid material.The as-synthesized V_2O_5 with about 100 nm in diameter and several hundreds nanometers in length were obtained and PPy layer with about 100 nm in thickness coated on the surface of V_2O_5. Electrochemical measurement showed that V_2O_5@PPy hybrid material had improved lithium storage ability and cycling performance compared with pure V_2O_5. PPy modification supplied a new route to obtain V_2O_5 hybrid cathode with significantly improved cyclic performance and showed promising applications in recharged lithium batteries.

Keywords Vanadium pentoxide · Polypyrrole · Recharged lithium battery · Cyclic performance

1 Introduction

The development of cathode materials with high specific capacity and high energy density [1] still is main research tendency in the field of rechargeable lithium-ions batteries (LIBs). Many cathodes formed from transition metal oxides (Mn, V, Cr, Ni, Co, Fe, et al.) demonstrate high specific capacity and high energy density [2–8]. The diffusion of Li^+ within the cathodes is an important factor when new cathode or hybrid materials were designed. In addition, the electronic conductivity of these materials is quite low, which usually can be improved by carbon coating and doping technologies [9–12].

Besides, conducting polymers, such as polypyrrole (PPy), polyaniline and poly (3, 4-ethylene dioxythiophene), for their high electronic/ionic conductivity and lithium storage ability, were also studied as candidates for the development of rechargeable lithium batteries [13–15], while lows specific energy hindered their applications. Therefore, hybrid organic–inorganic materials based on conducting polymers and transition metal oxides represent an opportunity to take advantage of the best properties of each type of material.

Vanadium pentoxide (V_2O_5) has been studied as cathode material for its lamellar structure and high specific discharge capacity for more than one decade. But the bad cyclic performance limited its application as cathode. Therefore, abundant attempts focused on designing V_2O_5/conducting polymer hybrid materials as a cathode in lithium-ion batteries [16–20]. Boyano et al. [21] reported PPy/V_2O_5 hybrid materials synthesized in different acidic solution using PSA as an organic additive, and the lithium storage performance of PPy/V_2O_5 hybrid cathode synthesized with $HClO_4$ as proton acid of PPy polymerization was significantly improved. Kuwabata et al. [22] have synthesized PPy/V_2O_5 composites by chemical polymerization of pyrrole (Py) using V_2O_5 powder dispersed in $HClO_4$ solution as oxidizing agent. Nilofar et al. [23] synthesized core-shell PANI/V_2O_5 nanocomposite by microemulsion method in the host of inorganic matrix with methyl orange (MO)/$FeCl_3$ as a reactive self-degraded soft-template. Cui et al. [24] synthesized core-shell PPy/V_2O_5 by in-suit chemical oxidation polymerization of pyrrole in the host of inorganic matrix and PPy layer with 30–50 nm coated on the surface of long nanotube, while the lithium storage was not researched.

H. Zhao · A. Yuan · B. Liu · S. Xing · X. Wu · J. Xu (✉)
College of Science, Shanghai University,
Shanghai 200444, China
e-mail: xujiaqiang@shu.edu.cn

In the present study, micro–nanosized V_2O_5 was synthesized by hydrothermal reduction of V_2O_5 with cetyltrimethyl ammonium bromide (CTAB) as directing template and reductant. Followed, V_2O_5@PPy hybrid cathode was synthesized by in situ polymerization of Py monomer on the surface of micro–nanosized V_2O_5 in diluted acid aqueous without any other oxidant, and improved electrochemical performance were expected. Environmental friendly of the synthesis route, high charge/discharge capacity and enhanced cycling performance of V_2O_5@PPy indicated promising applications as cathode material in LIBs.

2 Experimental

2.1 Preparation of V_2O_5 and V_2O_5@PPy composite

Analytic purified V_2O_5, pyrrole, CTAB, and diluted chlorhydric (HCl) and hydrogen peroxide are purchased from Sinopharm Chemical Reagent Co,Ltd. China.

Preparation of V_2O_5 and V_2O_5@PPy composite are as followed. 0.9117 g commercial amorphous V_2O_5 and 2.191 g CTAB were dispersed into 40 mL DDI water and kept vigorously stirred for 3 h at room temperature. The obtained yellow slurry was removed to 50 mL Teflon kettle, and the volume of slurry is about 80–90% of the whole volume. Then, the kettle was kept at 180 °C for 48 h. After cooled to room temperature, a precipitate was obtained at the bottom of kettle. Washed by ethanol and DDI water for several times to remove impurities, the filter cake was dried in 80 °C for 12 h and a black precursor was obtained. Followed, a part of black precursor was heated in furnace at 450 °C for 2 h and V_2O_5 was obtained.

To prepare V_2O_5@PPy, 100 mg as synthesized V_2O_5 was dispersed into 100 mL DDI water by ultrasonic for 20 min, then 1 mL 0.1 M HCl aqueous was added into the suspension and kept violently stirring for 5 min. Followed, 5 mL water–ethanol with 12 mg Py monomer was added into the suspension and kept stirring for 3 h. Finally, the suspension was centrifuged and washed with DDI water and ethanol for several times. The black powder was dried at 60 °C for 24 h. The obtained powder was named as V_2O_5@PPy composite.

As a reference, pure PPy was synthesized by chemical oxidation of pyrrole as followed: 200 mg pyrrole monomer was added into 100 mL DDI water–ethanol solution (v/v = 1:1) and kept stirring for 30 min with N_2 protection. Then, 5 mL hydrogen peroxide (3 wt%) and 5 mL 0.1 M HCl were dropped into the former solution and kept stirring for 3 h. Finally, the suspension was centrifuged and washed with DDI water and ethanol for several times. The black powder was dried at 60 °C for 24 h in vaccum oven. The obtained powder was pure PPy.

2.2 Characterization of materials

X-ray powder diffraction (XRD) data were collected using a Rigaku DLMAX-2550 V diffractometer (40 kV, Cu Kα ($\lambda = 1.54056$ Å); 2θ range 10–90°; scan speed of 5°/min). The morphology of cathode materials was characterized by scanning electron microscope (SEM) (JEOL JSM-6700F) and transmission electron microscope (TEM) (JEM-2010F). Fourier transform infrared spectroscopy (FTIR) was carried out on Avatar 370 in the wave length ranges from 450 to 2000 nm^{-1} to determine the existence of PPy (1.91 cm^{-1} resolution is available). Inductively coupled plasma atomic emission spectrometer (ICP-AES) was used to quantify the content of vanadium element in the V_2O_5@PPy composites after the sample was dissolved in concentrated hydrochloric acid.

2.3 Electrochemical characterization

Electrochemical studies were performed with a potentiostat–galvanostat system (CT 2001A, LAND, Wuhan, China) under a constant current density to charge-discharge at C/40 in the 2–4 V range. The electrochemical performances were evaluated with CR2016 coin cells assembled with the cathodes thus fabricated, metallic lithium cathodes in a glove box (Universal series, Mikrouna, Shanghai, China). 80 mg of cathode material and 10 mg acetylene black were mixed into 500 μL 20 mg mL^{-1} PVDF in N-methylpyrroidinone and the slurry was stirring for 8 h. The suspension was coated on an aluminum current collector by a scraper (200 μm) and dried at 80 °C in vacuum oven for 12 h, then it was cut to a 9 mm diameter discs as cathode. A solution of $LiPF_6$ in EC/DMC/DEC (1:1:1 in weight) (Guotaihuarong LTD., Zhangjiagang, China) was used as electrolyte. The separator (Celgard 2400, microporous polypropylene membrane) was purchased from Celgard Inc. The pure V_2O_5 and VO_2 electrode material was mixed with 10% of carbon as conducting material, respectively. Cyclic voltammery (CV) were carried out on Solartron 1287 electrochemical interface + 1255B frequency analyzer. CV curves were obtained between 2 V to 4 V vs Li^+/Li with scan speed of 0.0001 V s^{-1}.

3 Results and discussion

SEM and TEM images of the synthesized V_2O_5 and V_2O_5@PPy composite are shown in Fig. 1. V_2O_5 obtained by hydrothermal reduction of CTAB and high temperature treatment has micro–nanosized rod structure with about 700 to 1,000 nm in length and 300 to 500 nm in diameter (Fig. 1a). As for V_2O_5@PPy (Fig. 1b), the dark region was assigned to V_2O_5 with 700 nm in length and 250 nm in diameter. The light color region is PPy layer with thickness

of about 100 nm. SEM image of V_2O_5 (Fig. 1c) is corresponding to that of TEM and a smooth and clean surface was observed. As for the SEM image of V_2O_5@PPy (Fig. 1d), an obscure surface was observed due to the low conductivity of amorphous PPy coated on the surface of V_2O_5. These results confirm that a successful synthesis we design to prepare V_2O_5@PPy composite.

Scheme of the synthesis route of V_2O_5@PPy composite is illustrated in Fig. 2. With CTAB as directing template and reductant in hydrothermal condition, micro–nanosized V_2O_5 was obtained after the hydrothermal precursor was heated at 450 °C in air for two hours. V_2O_5 has moderately oxidability and it can quickly oxidize Py to PPy in room temperature. In our study, diluted HCl was dropped into the suspension of V_2O_5/water, and the acidic species of V_2O_5 played as oxidant and proton acid of polymerization of Py. Quickly oxidation of Py occurred on the surface of V_2O_5 and a core-shell-like structured V_2O_5@PPy composite was obtained by in situ polymerization method. The reaction between V_2O_5 and HCl was not observed which usually occurred in concentrated HCl solution, the reason maybe due to the very low concentrate of HCl we used.

XRD patterns (Fig. 3) confirmed that V_2O_5 was successfully prepared by hydrothermal reduction of commercial V_2O_5 with CTAB as reduced agent, followed with high temperature treatment. V_2O_5 with high crystallinity and uniformity was synthesized. Indexing by standard diffraction

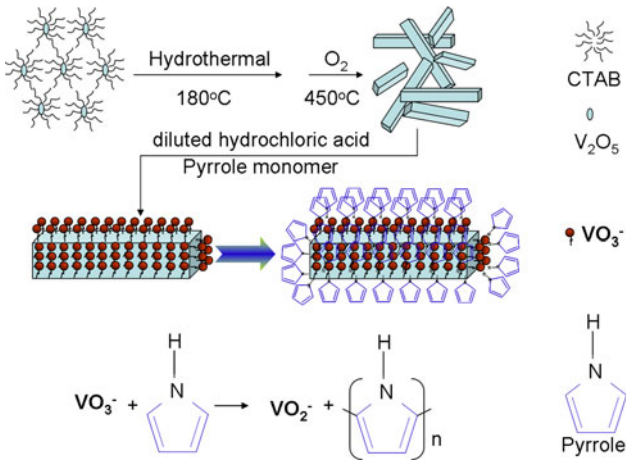

Fig. 2 Scheme of synthesis of V_2O_5@PPy composite

card (PDF#41-1426), XRD patterns of as synthesized vanadium oxide was identical to that of α-V_2O_5 [25, 26]. As for V_2O_5@PPy, V_2O_5 still kept well crystallinity and the positions of diffraction peaks have no obvious change. This indicated that PPy did not change the crystallinity of V_2O_5 and no chemical interaction between V_2O_5 and PPy. No obvious PPy diffraction peak was found because amorphous PPy usually shows a broad and weak diffraction peak and the overlapped diffraction peaks between PPy and V_2O_5 at about 25°. The increase of weight and the color change of suspension from yellow to dark after Py immersed in acidic V_2O_5

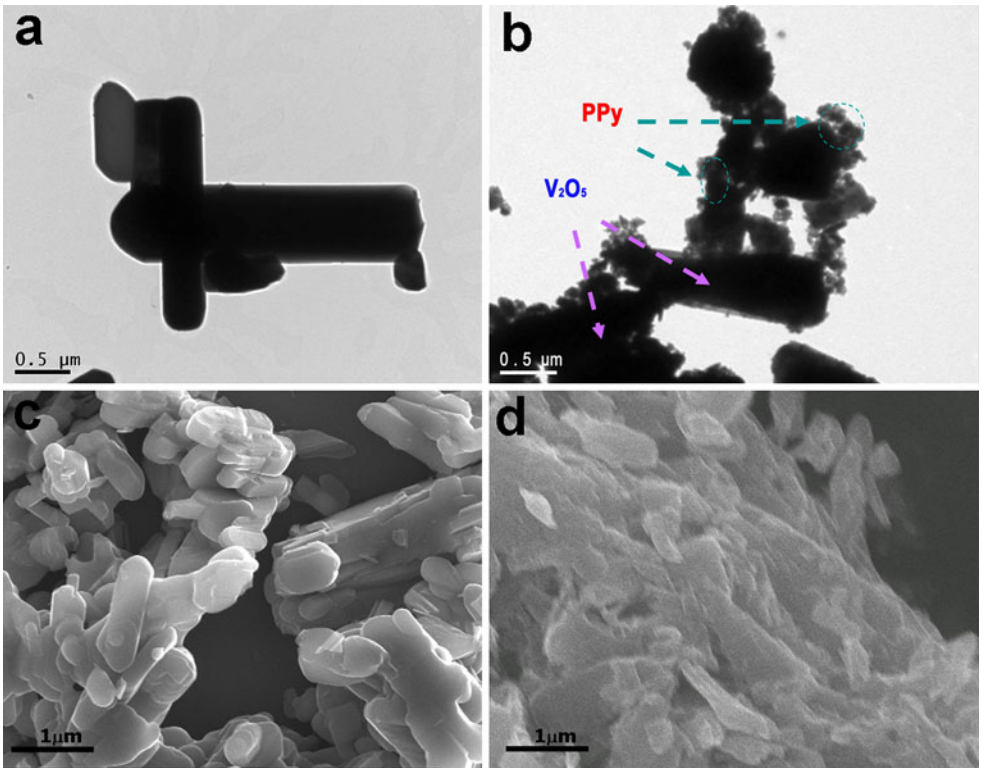

Fig. 1 TEM and SEM images of V_2O_5 (**a**, **c**) and V_2O_5@PPy composite (**b**, **d**)

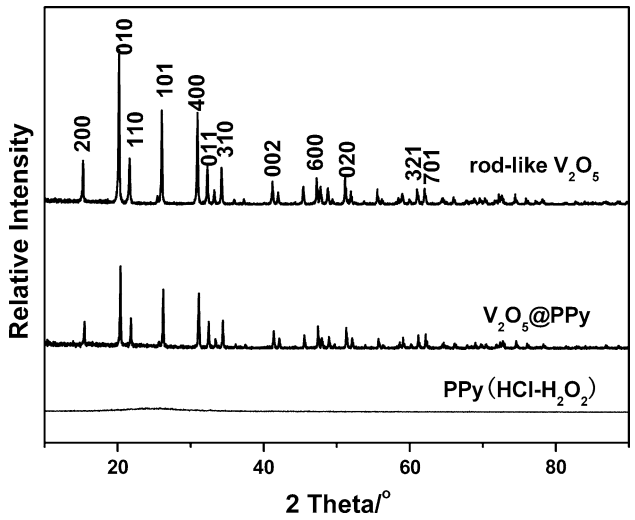

Fig. 3 XRD patterns of V_2O_5, V_2O_5@PPy composite and PPy obtained by chemical oxidation with hydrogen peroxide as oxidant and diluted hydrochloric acid as proton acid

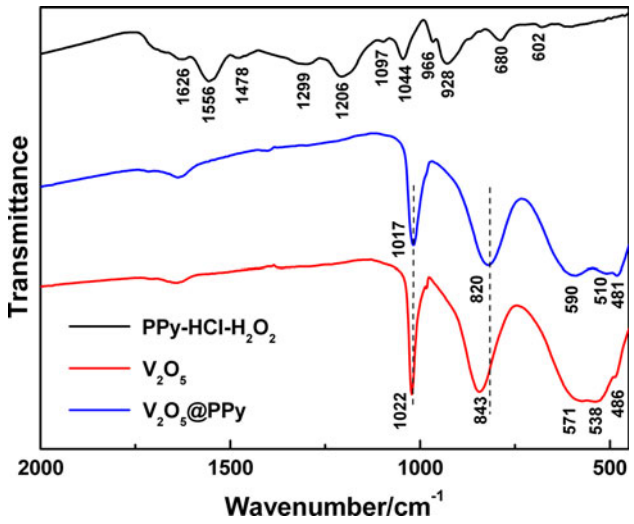

Fig. 4 FTIR spectra of V_2O_5, PPy, and V_2O_5@PPy composite

indirectly confirmed that a reaction between Py and acidic V_2O_5 occurred. Therefore, PPy was successfully polymerized on the surface of V_2O_5 with acidic V_2O_5 as oxidant. ICP-AES results showed that vanadium oxides in the V_2O_5@PPy composite was 88%, which is corresponding to the stoichiometric proportion of raw materials. The particle size of V_2O_5 in V_2O_5 and V_2O_5@PPy calculated by Scherrer equation was about 76 and 74 nm, respectively (calculated with FWHM of the V_2O_5 (010) lattice).

FTIR spectra were illustrated in Fig. 4 to evaluate the existence of PPy in the V_2O_5@PPy hybrid material. As shown in Fig. 4, characteristic adsorption peaks of PPy at 1299 cm^{-1} and 1026 cm^{-1} were ascribed to in-plane C–H stretching vibration and in-plane N–H deformation, respectively. The bands at 966 cm^{-1} usually reflected the C–N stretching vibration. The frequencies at 1,556 and 1,448 cm^{-1} were attributed to the antisymmetric and symmetric pyrrole ring vibration. The spectrum of the α-V_2O_5 displayed in Fig. 4 is characterized by three absorption bands centered at 1,022, 843, and 571 cm^{-1}. First band at 1,022 cm^{-1} is assigned to the V = O stretching (vanadyl oxygen), the last two at 843 and 571 cm^{-1} are due to V–O–V deformation modes. For V_2O_5@PPy composite, the characteristic peaks belonging to PPy was not observed obviously because of its low relative content. The V–O–V vibration at 843 and 571 cm^{-1} shifted to 820 and 590 cm^{-1}, which indicated a sensitive physical interaction between V_2O_5 and PPy. Therefore, we roughly thought that PPy was oxidized by V_2O_5 in diluted HCl and polymerized successfully [21, 24, 27].

Electrochemical properties of as synthesized V_2O_5 and V_2O_5@PPy composite for Li-ion battery applications were evaluated using galvanostatic charge/discharge (Fig. 5). Two lithium ions were inserted into the crystalline of V_2O_5 and V_2O_5@PPy step by step and three pairs of obvious plateaus were observed at around 2.55/2.35 V, 3.30/3.25 V, and 3.60/3.51 V in the initial charge/discharge cycle, which usually is attributed to 0.5 Li^+, 0.5 Li^+, and 1 Li^+ insertion/extraction, respectively. The charge/discharge curves of as

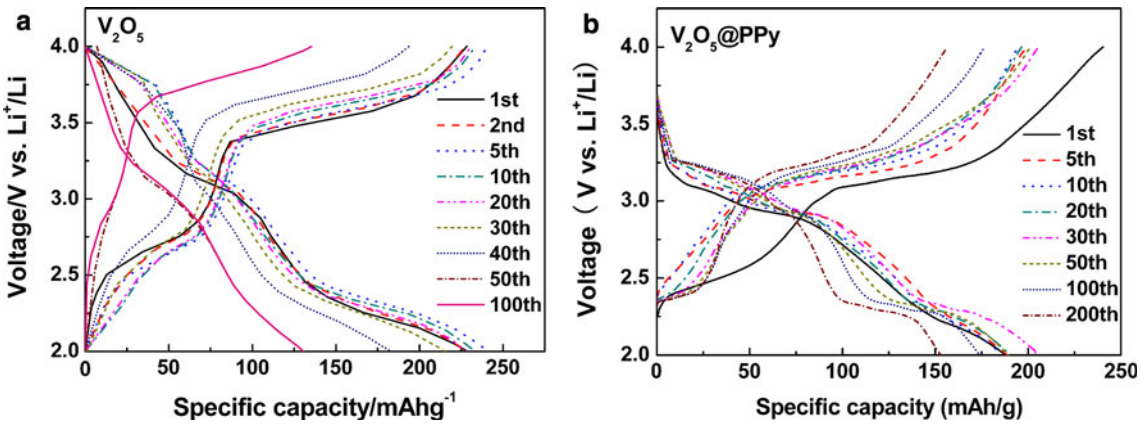

Fig. 5 Electrochemical performance of V_2O_5 (**a**) and V_2O_5@PPy (**b**) electrode at the charge/ discharge ratio of C/40

obtained V_2O_5 and V_2O_5@PPy cathodes showed a multi-step process due to theirs structural changes upon the Li^+ ions insertion/extraction process. The electrochemical reaction between V_2O_5 and metal lithium can be described as followed [28–30]:

$$V_2O_5 + 0.5\ Li^+ + 0.5e^- \leftrightarrow Li_{0.5}V_2O_5 \quad (1)$$

$$Li_{0.5}V_2O_5 + 0.5\ Li^+ + 0.5e^- \leftrightarrow LiV_2O_5 \quad (2)$$

$$LiV_2O_5 + 1\ Li^+ + 1e^- \leftrightarrow Li_2V_2O_5 \quad (3)$$

The theoretical specific capacity of V_2O_5 when two Li^+ ions insert/extract is about 295 mAh g^{-1}. Figure 5 depicted the curves of discharge capacity after different charge/discharge cycle for the V_2O_5 and V_2O_5@PPy electrodes with charge/discharge ratio of C/40 at 25 °C. The initial specific capacity of V_2O_5 and V_2O_5@PPy cathodes is 241 and 208 mAh g^{-1}, respectively. About 82 and 69% of theoretical lithium storage capacity was obtained, which indicated potential application as cathode of LIBs. Big electrochemical polarization of V_2O_5@PPy electrode in the initial cycles maybe attributed to that of the PPy layer, which limited the lithium ion diffusion and more Li ions were consumed in the formation process of solid electrolyte interface membrane. Three pairs of charge/discharge plateaus at 3.3/3.1, 3.1/2.9, and 2.4/2.3 V were observed from V_2O_5@PPy electrode, which is according to that 0.5 Li, 0.5 Li, and 1 Li insertion/extraction in different electrochemical step, respectively. In case of pure V_2O_5 electrode, the two plateaus at about 3.2 and 3.0 V mixed together and the plateaus at around 2.4 V is obvious, which indicated different reversibility in the Li insertion/extraction. Compared with pure V_2O_5 electrode, V_2O_5@PPy electrode showed clearer plateaus and bigger charge/discharge capacity, indicated improved reversibility.

The cyclic performance of V_2O_5 and V_2O_5@PPy electrodes was shown in Fig. 6. All the two electrodes showed an active process in the initial several cycles. Fast capacity decay of V_2O_5 electrode was observed after 50 cycles and the discharge capacity is about 130 mAh g^{-1} after 100 cycles charge/discharge, about 46% of the initial capacity was kept. The reason maybe attribute to the collapse of

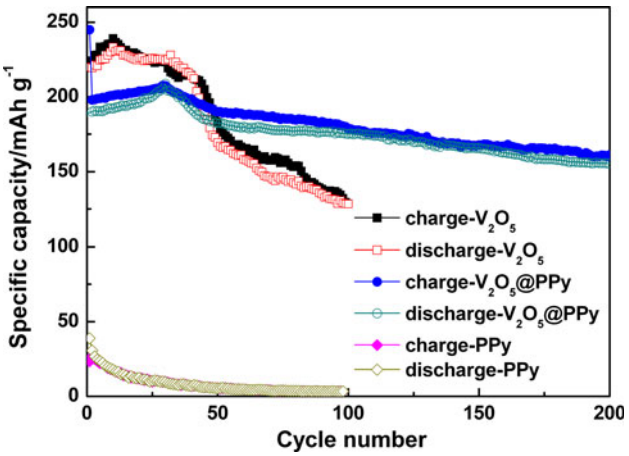

Fig. 6 The plots of capacity vs. cycle number with V_2O_5, V_2O_5@PPy, and PPy as cathode, respectively

V_2O_5 or the formation of irreversible phases in the charge/discharge process. While for V_2O_5@PPy electrode, a slow capacity increase to about 210 mA h g^{-1} before 30 cycles and a slow decay occurred only 17% decay of initial discharge capacity was found. After 100 cycles charge/discharge, about 170 mAh g^{-1} of the discharge capacity still was kept in V_2O_5@PPy electrode, which confirmed significantly enhanced cyclic performance after PPy coating on the surface of V_2O_5. As a reference, the lithium storage of PPy was studied by assembling coin cell battery with PPy as cathode. As shown in Fig. 6, the initial capacity of PPy is about 40 mAh g^{-1}. After 25 cycles, the capacity decayed to about 20 mAh g^{-1} and kept stabled capacity of 17 mAh g^{-1} after 50 cycles. These results confirmed that the contribution of PPy to the total capacity is small, while its role on improving the cyclic performance of V_2O_5 is very significant.

The electrochemical reaction mechanism was studied by CV technology. As shown in Fig. 7, at least three pairs of redox peaks were observed in the range of 2.0 to 4.0 V, which represents 0.5 Li, 0.5 Li, and 1 Li insertion/extraction in different step, respectively. This result is corresponding to that of Eqs. 1–3 and the initial charge/

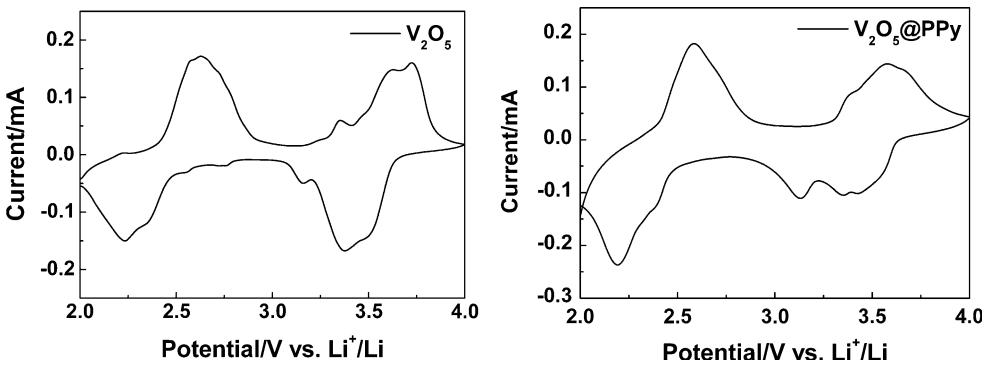

Fig. 7 Cyclic voltammery of V_2O_5 and V_2O_5@PPy electrodes

discharge curves in Fig. 5. Moreover, the peak potential of V_2O_5@PPy electrode at around 3.4 V is a bit smaller than that of V_2O_5 electrode, indicating more reversibility than that of pure V_2O_5.

The improved cyclic performance of V_2O_5@PPy electrode can be illustrated as followed: First, in situ polymerization of PPy on the surface of V_2O_5 supplied close electrical contact between PPy and V_2O_5 at the nanoscaled level around the outside of V_2O_5; second, the kinetics of Li insertion/extraction and the lithium storage performance can be expected to be improved in this V_2O_5@PPy composite over those of conventional materials. Third, the PPy layer on the surface of V_2O_5 should plays a role of plastic protecting shell and the collapse of V_2O_5 due to volume expansion during the charge/discharge process can be prevented effectively.

4 Conclusions

Micro–nanosized vanadium pentoxide with high electrochemical capacity was synthesized by hydrothermal reduction with CTAB as direct template and reductant, followed by thermal treatment in air. PPy in-situ polymerization on the surface of V_2O_5 improved the electrochemical cyclic performance of V_2O_5. Electrochemical measurement showed that V_2O_5@PPy hybrid material had high lithium storage ability and the initial specific discharge capacity in the voltage range of 2–4 V was 208 mAh g^{-1}. After 200 cycles charge/discharge, more than 170 mAh g^{-1} discharge capacity was still kept. While the discharge capacity of V_2O_5 without PPy descended to 130 mAh g^{-1} after 100 cycles charge/discharge process. PPy modified V_2O_5 significantly improved the cyclic performance of V_2O_5 and showed promising applications in LIBs.

Acknowledgments We acknowledge the financial support from the National Natural Science Foundation of China (Grant No. 61071040), Leading Academic Discipline Project of Shanghai Municipal Education Commission (No.J50102), and Innovative Foundation of Shanghai University. We also thank Instrumental Analysis & Research Center of Shanghai University, China, for samples characterization.

References

1. Aricò AS, Bruce PG, Scrosati B, Tarascon JM, van Schalkwijk W (2005) Nat Mater 43:66
2. Guyomard D, Tarascon JM (1992) J Electrochem Soc 139:937
3. Sakurai Y, Yamaki J (1988) J Electrochem Soc 135:791
4. Grugeon S, Laruelle S, Dupont L, Chevallier F, Taberna PL, Simon P, Gireaud L, Lascaud S, Vidal E, Yrieix B, Tarascon JM (2005) Chem Mater 4:5041
5. Padhi AK, Nanjundaswamy KS, Goodenough JB (1997) J Electrochem Soc 144:1188
6. Xia Y, Yoshio M (1997) J Electrochem Soc 144:4186
7. Padhi AK, Nanjundaswamy KS, Masquelier C, Goodenough JB (1997) J Electrochem Soc 144:2581
8. Masquelier C, Padhi AK, Nanjundawsamy KS, Goodenough JB (1998) J Solid State Chem 135:228
9. Yun NJ, Ha HW, Jeong KH, Park HY, Kim K (2006) J Power Sources 160:1361
10. Zhuang D, Zhao X, Xie J, Tu J, Zhu T, Cao G (2006) Acta Phys Chem 22:840
11. Liu H, Fu LJ, Zhang HP, Gao J, Li C, WuP YP, Wu HQ (2006) Electrochem Solid-State Lett 9:529
12. Ravet N, Chourinard Y, Magnan JF, Besner S, Gauthier M, Armand M (2001) J Power Sources 97–98:503
13. Kim Y, Ta QT, Dinh HC, Aum PK, Yeo IH, Cho WI, Mho S (2011) J Electrochem Soc 158:133
14. Osaka T, Momma T, Nishimura K, Kakuda S, Ishii T (1994) J Electrochem Soc 141:1994
15. Neves S, Polo Fonseca C (2002) J Power Sources 107:13
16. Park NG, Ryu KS, Chang SH (2002) J Power Sources 103:273
17. Demetz GF, Anaissi FJ, Toma HE (2000) Electrochim Acta 46:547
18. Huguenin F, Gitotto EM, Buttry DA (2002) J Electroanal Chem 536:37
19. Kang SG, Kim KM, Chang SH (2004) J Power Sources 133:263
20. Goward GR, Loroux F, Nazar LF (1998) Electrochim Acta 43:1307
21. Boyano I, Bengoechea M, de Meatza I, Miguel O, Cantero I, Ochoteco E, Rodríguez J, Lira-Cantú M, Gómez-Romero P (2007) J Power Sources 166:471
22. Kuwabata S, Masui S, Tomiyori H, Yoneyama H (2000) Electrochim Acta 46:91
23. Asim N, Radiman S, Bin Yarmo MA (2008) Mater Lett 62:1044
24. Cui L, Li J, Zhang XG (2009) Mater Lett 63:683
25. Pinna N, Willinger M, Weiss K, Urban J, Schlögl R (2003) Nano Lett 1131:3
26. Cao AM, Hu JS, Liang HP, Wan LJ (2005) Angew Chem Int Ed 4391:44
27. Kim Y, Thieu M.-T, Yeo I.-H, Cho W.-I, Mho S. Meet. Abstr.-Electrochem. Soc./MA2009-01/B1-Battery/Energy Technology Joint General Session
28. Tranchant A, Messina R, Perichon J (1980) J Electroanal Chem 225:113
29. Benmoussa M, Outzourhit A, Bennouna A, Ameziane EL (2002) Thin Solid Films 11:450
30. Kim Y-T, Gopukumar S, Kim K-B, Cho B-W (2003) J Power Sources 110:117